치의과학박사 학위논문

# Effect of labiopalatal position of an implant on stress and displacement in bone: a 3-dimensional finite element analysis

## 임플란트의 순구개 위치가 골의 응력과 변위에 미치는 영향: 3차원 유한요소분석

2019 년 2 월

서울대학교 대학원

치의과학과 치과보철학 전공

박 철 우

Abstract

# Effect of labiopalatal position of an implant on stress and displacement in bone: a 3-dimensional finite element analysis

**Cheol-Woo Park**, D.D.S., M.S.D.

Department of Prosthodontics, Graduate School, Seoul National University

(Directed by Professor **Jung-Suk Han**, D.D.S., M.S., Ph.D.)

**Purpose:** The aim of this study was to investigate the effects of labiopalatal position of an immediately loaded implant on stress and displacement of surrounding bone in the anterior maxilla using three-dimensional finite element analysis.

**Materials and methods:** Five simplified three-dimensional finite element models, consisting of an internal connection-type implant (4.0 × 10.0 mm), a customized abutment, and a cemented zirconia crown of the central incisor, were constructed. These implants

were inserted into five different labiopalatal positions, located 0.5 mm (P1) and 1.0 mm (P2) palatally from the center, at the center (C), and 0.5 mm (L1) and 1.0 mm (L2) labially from the center of the crestal cortical bone. An oblique static load of 178 N was applied to the palatal surface of the zirconia crown at an angle 30° to the long axis of the implant under immediate and delayed loading conditions. The von Mises stress and displacement of the surrounding bone were calculated at the bone-implant interface and at the surface of the labial bone.

**Results:** The von Mises stresses were mainly concentrated on the crestal cortical bone around the implant platform and neck. Stress distributions on the labial cortical bone increased with more labial positioning of the implants. The stresses in cancellous bone were more evenly distributed under conditions of immediate than delayed loading. The maximum stresses on cortical bone were regularly related to the labiopalatal positions of the implant at the labial bone surface, but not at the bone-implant interface. Under immediate loading conditions, the P1 and C models showed favorable stress and displacement patterns in the cortical bone. The maximum displacement increased as implants were placed more labially, but differed little between immediate and delayed loading conditions. The maximum displacement at the bone-implant interface was 33.44 μm under immediate loading condition.

**Conclusions:** The labiopalatal position of an implant affected the von Mises stress and displacement of surrounding bone in the anterior maxilla. Immediate loading of an implant in the center or on the palatal side of the crestal cortical bone resulted in favorable stress and displacement patterns in surrounding bone.

**Keywords**: Dental implant, Immediate loading, Labiopalatal position, Finite element analysis

**Student Number:** 2011-31175

# Effect of labiopalatal position of an implant on stress and displacement in bone: a 3-dimensional finite element analysis

**Cheol-Woo Park**, D.D.S., M.S.D.

Department of Prosthodontics, Graduate School, Seoul National University

(Directed by Professor **Jung-Suk Han**, D.D.S., M.S., Ph.D.)

## CONTENTS

# I. INTRODUCTION

Implant-supported prostheses have been widely used to replace missing teeth because of their proven functional, biological, and mechanical advantages, as well as their long-term clinical success rates [1]. Brånemark's classical loading protocol requires the implant to be covered with gingiva during an osseointegration period of 3–6 months without loading. However, improvements in the design and surfaces of implants, along with patient demands for shorter treatment periods, have led to the increased use of immediate loading rather than classical loading protocols [2, 3].

Immediate loading is defined as a provisional or definitive restoration within 48 hours after implant placement [4-5]. Immediate loading protocols can reduce overall treatment times and the number of operations, while improving soft tissue healing by providing prosthetic support. In addition to providing satisfactory aesthetic and psychological outcomes, immediate loading was shown to be reliable and successful in providing stable implants for the restoration of missing teeth [6-10].

Satisfactory aesthetic outcomes of prosthetic implants in the anterior maxilla require that the implants be inserted into their proper three-dimensional position [11]. The labiopalatal position of the implant influences the emergence profile of the prosthesis, as well as labial bone thickness [12, 13]. An implant positioned too labially can result in resorption of labial bone and gingival recession [14], whereas an implant positioned too palatally can result in

occlusal and esthetic problems as well as difficulties managing oral hygiene. Labial bone thickness is an important determinant of long-term implant success, as determined by maintenance of labial bone and aesthetic outcomes of soft tissue [15], with a labial bone thickness of 2 mm reported necessary to avoid vertical bone resorption and maintain appropriate soft tissue support [16, 17].

The bone quality of the anterior maxilla is usually inferior to that of the mandible, and maxillary incisors are positioned obliquely to the occlusal force [18, 19]. Thus, the long-term success of implantation is largely dependent on the biomechanical environment, regardless of loading protocols [20, 21]. An immediately loaded implant subjected to excessive force may fail early in the healing phase. Application of excessive force to an osseointegrated implant may causes loss of surrounding bone and result in late failure of the implant [22]. Thus, application of excessive force to an implant-supported prosthesis during the first healing period may result in micromotion, which may ultimately cause fibrous encapsulation at the bone-implant interface [23-25]. A mechanical stress level exceeding the tolerance of bone can cause bone resorption, which may lead to implant instability.

Finite element analysis (FEA) is a computational numeric method that assesses stresses and strains in mesh structures. For example, FEA has been used to predict biomechanical behaviors of bones surrounding dental implants and to evaluate the contribution of clinical factors to implant success [26]. Three-dimensional (3D) FEA has also been used in

biomechanical studies that simulate implant loading conditions and insertion torque [27, 28]. FEA has been utilized in studies assessing the effects of the apicocoronal position of an implant on bone stability and in morphological analyses of labial bone thickness around the implant [29, 30]. To our knowledge, however, FEA has not been used to assess the relationship between the labiopalatal position of an immediately loaded implant with insertion torque and the biomechanical behavior of surrounding bone.

The aim of this study was to utilize FEA to assess the effect of the labiopalatal position of an immediately loaded implant on the stress and displacement of surrounding bone in the anterior maxilla. The null hypothesis was that the labiopalatal position of an immediately loaded implant would not affect the distribution and magnitude of stress and displacement.

# II. MATERIAL AND METHODS

## 2.1. Model construction

Implants were inserted into five different labiopalatal positions in a partially edentulous healed ridge and restored with a customized abutment and a zirconia crown for immediate or delayed loading in the anterior maxilla.

Images obtained by cone-beam computed tomography (CBCT; CS9300, Carestream Dental LLC, Atlanta, GA, USA) were used by OnDemand3D software 1.0.10.5385 (Cybermed, Inc., Seoul, Korea) to reconstruct a 3D virtual model of the maxilla. The reconstructed model was transformed to a simplified bone model using Altair HyperWorks software 13 (Altair Engineering Inc., Troy, MI, USA). The model was designed to have an inferosuperior height of 22.0 mm, a mesiodistal length of 20.0 mm, a labiopalatal width of 7.3 mm, and a uniform cortical bone thickness of 0.75 mm surrounding the cancellous bone, yielding a D3 bone (Fig. 1) [31, 32]. A solid model of an internal connection-type tapered and threaded IS III active implant (Neobiotech Co., Ltd., Seoul, Korea), of diameter 4.0 mm (maximum 4.3 mm) and length 10.0 mm was used. A customized abutment and a zirconia crown were designed using Exocad software 6136 (Exocad GmbH, Darmstadt, Germany), based on the position coordinates of an implant determined by CBCT (Fig. 2).

Each of the five finite element models used in this study consisted of a simplified bone model, an implant, a customized abutment, an abutment screw, and a crown. Using a

numerical analysis program, Altair HyperWorks version 13 (Altair Engineering Inc., Troy, MI, USA), the implant was inserted at the level of the crestal cortical bone in different labiopalatal positions, with the central axis of the implant located 1.0 mm (P2 model) and 0.5 mm (P1 model) palatally, at the center (0 mm; C model), and 0.5 mm (L1 model) and 1.0 mm (L2 model) labially relative to the central vertical axis of the bone model (Table 1 and Fig. 3).

The finite element models were discretized with tetrahedral elements of various sizes to create a mesh (Fig. 4). To allow more accurate analyses, the regions in the vicinity of each bone-implant interface and cortical bone were meshed with finer elements of size 0.10–0.15 mm. The total number of elements ranged from 1,274,419 to 1,394,707 and the total number of nodes from 249,299 to 255,605.

## 2.2. Material properties

To simplify calculations, all materials used in this study were assumed to be homogeneous, isotropic, and linearly elastic. Based on previous findings [32, 33], Young's modulus and Poisson's ratio were determined to be 13.7 GPa and 0.3, respectively, for cortical bone; 1.37 GPa and 0.3, respectively, for cancellous bone; 110 GPa and 0.35, respectively, for titanium alloy; and 200 GPa and 0.31, respectively, for zirconia (Table 2).

## 2.3. Contact conditions

The contact conditions at the bone-implant interface were constructed as described [34]. For immediate loading, the bone-implant interface was constructed using nonlinear frictional contact elements with a friction coefficient (μ) of 0.3, resulting in a non-osseointegrated frictional surface. Frictional contact allowed for minor displacement without interpenetration. For delayed loading, the bone-implant interface was regarded as a completely fixed contact simulating 100% osseointegration (Fig. 5A). In addition, the interfaces among the components of the implant (*i.e.*, the implant itself, the abutment screw, and the customized abutment) were regarded as frictional contacts (μ=0.3), whereas the interfaces of cortical bone with cancellous bone and the customized abutment and crown were regarded as fully fixed (Fig. 5B).

## 2.4. Boundary and loading conditions

Boundary conditions included constraints at all six degrees of freedom at each of the nodes located on the mesial and distal exterior surfaces of the bone model. The displacement components of the nodes were set to zero [18, 19] (Fig. 6A). An oblique static load of 178 N, the average bite force at the incisors [35, 36], was applied to a node on the palatal surface 2 mm vertically from the incisal ridge of the zirconia crown, at a 30° angle to the long axis of the implant [18] (Fig. 6B).

## 2.5. Application of insertion torque

An insertion torque of 35 Ncm was applied in the finite element model to simulate the clinical situations of immediate loading. Based on previously reported method [28], the magnitude of deformation of cortical bone and cancellous bone was determined to be 2.38 μm and 6.50 μm, respectively. The meshes of bone were offset to the inside of the implant by the calculated magnitude of force-induced deformation along the bone-implant interface. The interfacial bone nodes were forced outwards by the same magnitude of deformation. After contact conditions were achieved at the bone-implant interface, an analysis was performed at the time of static equilibrium.

## 2.6. Finite element analysis

FEA of each model was performed using Virtual Performance Solution software 2016.1 (ESI Group, Paris, France), followed by post-processing with Visual-Viewer software 13.0 (ESI Group, Paris, France). The von Mises stress and displacement of the bone around the implant were calculated. The resulting distribution patterns of stress and displacement were compared visually using contour plots. The effect of the labiopalatal positions of an immediately loaded implant was analyzed by comparing the maximum values of von Mises stress and displacement calculated at the bone-implant interface and the labial bone surface on the labiopalatally perpendicular plane that included the central axis of the implant.

# III. RESULTS

## 3.1. von Mises stress analysis

### 3.1.1. Bone-implant interface under delayed loading conditions

Under conditions of delayed loading, the von Mises stresses were concentrated on the labial side of the crestal cortical bone around the implant platform, with less stress on the palatal side of the neck and the apical area of the implant (Fig. 7). The stress distribution area in cortical bone increased as the implant was positioned more labially. Stress in the P2 and L2 models was also concentrated at the cortical bone adjacent to the thread tip around the implant neck. Maximum stresses were high in cortical bone, but low in cancellous bone (Table 3).

The maximum stress in cortical bone was higher in the P2, P1, and C models than in the L1 and L2 models. Maximum stress was lower in the P1 model (155.89 MPa) than in the P2 (157.57 MPa) and C (157.26 MPa) models, and was lowest in the L2 model (80.22 MPa). In all five models, maximum stress in the entire cortical bone was identical to that in the crestal cortical bone (Fig. 8).

All five models showed higher stress concentrations on the labial than on the palatal side of cancellous bone around the implant, especially, in the vicinity of the vertical surface between the implant threads. The models showed similar stress distributions according to the labiopalatal position of the implants. Maximum stress increased gradually from the P2

to the L1 model. Although maximum stress was highest for the L1 model (15.75 MPa), it was lowest for the L2 model (5.20 MPa).

### 3.1.2. Bone-implant interface under immediate loading conditions

Under conditions of immediate loading, the von Mises stresses were mainly concentrated on the labial side of the implant platform and on the crestal cortical bone around the implant neck. The stress distribution area in cortical bone increased as the implant was positioned more labially. The stress distribution patterns for more labial implants were similar to those observed under delayed loading conditions, but the stress concentration areas in the immediate loading models were above the interface between crestal cortical and cancellous bone (Fig. 9). In the P2 and L2 models, the stress was also concentrated in the area of cortical bone around the thread tip.

Of the five models, the C model showed the lowest maximum stress (133.82 MPa) on cortical bone. Maximum stress was observed on the labial side of the crestal cortical bone in the P1, C, and L1 models, but on the apical one-third area of the labial cortical bone in the L2 model. The P2 model showed the highest maximum stress (306.34 MPa) on the apical one-third area of the palatal cortical bone (Table 3). Maximum stresses on the entire cortical and crestal cortical bones were similar in the P1, C, and L1 models, but maximum stresses on the entire cortical bone were twice those on crestal cortical bone in the P2 and L2 models (Fig. 10).

All five models showed stress concentration on the surrounding cancellous bone along the implant thread, especially on the bone below the labial and above the palatal thread tips. All models showed higher maximum stresses under immediate than under delayed loading conditions. Maximum stresses decreased gradually from the P2 to the L2 model as the implant was positioned more labially.

### 3.1.3. Labial bone surface

Under delayed and immediate loading conditions, the stress distribution areas in cortical bone increased as the implant was positioned more labially (Fig. 7 and Fig. 9). From the P2 to the L2 model, the von Mises stresses became more concentrated on the marginal bone around the implant neck and were distributed widely toward the apical region. The maximum stresses gradually increased from the P2 to the L2 model under both delayed and immediate loading conditions (Table 4).

In all five models, maximum stresses were higher under immediate than under delayed loading conditions, regardless of the labiopalatal position of the implant. Maximum stress in the L2 model was twice that in the P2 and P1 models under immediate loading conditions, and twice that in the P2, P1, and C models under delayed loading conditions (Fig. 11).

## 3.2. Displacement analysis

In all models, displacement was greater on the labial side of the cortical bone around the implant platform, but less on the palatal side of the apical one-third area. From the P2 to the L2 model, the displacement area was greater on the labial side of the surrounding bone and was distributed more widely on the labial cortical bone toward the apical region under immediate than under delayed loading conditions (Fig. 12 and Fig. 13).

### 3.2.1. Bone-implant interface

Under immediate loading conditions, the L2 model showed the highest maximum (33.44 μm) displacement (Table 5). The maximum displacements in the P2 and P1 models were slightly lower under immediate than under delayed loading conditions, whereas maximum displacements in the C, L1, and L2 models were lower under delayed loading conditions (Fig. 14). In all models, the maximum displacement was observed at the interface between the labial edge of the implant platform and the crestal cortical bone.

### 3.2.2. Labial bone surface

Regardless of loading conditions, maximum displacement gradually increased from the P2 to the L2 model (Table 6). Displacement patterns were similar under immediate and delayed loading conditions, although maximum displacement was higher under immediate

loading conditions (Fig. 15). The maximum displacement was observed closer to the marginal bone around the implant platform from the P2 to the L2 model.

# IV. DISCUSSION

Implant-supported fixed prosthetic restorations were shown to be effective alternatives to conventional fixed partial prostheses or removable dentures in the restoration of missing teeth. These implant-supported restorations are regarded as definitive treatment because of their long-term successful osseointegration and predictable treatment outcomes. The accuracy of surgical guides has recently improved due to advances in CBCT, computer-aided design and manufacturing, and 3D printing technology, enabling the immediate loading of implants into the anterior maxilla [37, 38].

Immediately loaded implants are fixed into surrounding bone, without osseointegration, by mechanical engagement between the thread of the implant and bone. Primary stability at the time of implant placement is an important determinant of the long-term success or failure of implantation [39, 40]. Primary stability is dependent on bone quantity and quality, implant geometry, and surgical technique. The primary stability of immediately loaded implants into anterior maxilla with poor bone quality requires correct positioning of the implant with an appropriate insertion torque, such that the implant is surrounded by labial bone of adequate thickness [41]. An insertion torque of at least 32 Ncm has been reported to achieve osseointegration of immediately loaded implants in the esthetic zone [42, 43]. Immediate loading conditions in the present study were reproduced by application of an insertion torque of 35 Ncm in a finite element model.

The success of implant treatment is highly dependent on the method by which force applied to an implant is transmitted to the surrounding bone [44, 45]. Factors that may contribute to force transmission include implant diameter, length, position, angle, shape and surface characteristics; the implant-abutment connection method; the direction, magnitude, and frequency of the occlusal load; and the biomechanical characteristics of the bone-implant interface [18, 21, 26]. Excessive force leads to micromotion and bone resorption [22, 24]. In this study, an oblique static load of 178 N, the average bite force at the incisors [35, 36], was applied to a zirconia crown under both immediate and delayed loading conditions, with FEA used to assess the stress and displacement of surrounding bone according to the labiopalatal position of the implant.

The present study found that stress was concentrated on the labial side of the crestal cortical bone around the implant platform and neck. Maximum stress was greater on cortical than on cancellous bone in all five models, regardless of the loading conditions. These findings are in agreement with the results of previous FEA studies [18, 35, 45]. For example, von Mises stresses were found to be highly concentrated in cortical bone and widely distributed on the labial side of the cortical plate [28], and stresses were found to be concentrated on the cortical bone around the implant neck [46]. Stress was likely concentrated on cortical bone because this bone is much harder and has a more elastic modulus than cancellous bone [47]. Stress that exceeds the elastic limits of bone can lead to cortical bone resorption on the labial side of the anterior maxilla.

The present study found that the maximum stress at the cortical bone-implant interface was not proportional to the labiopalatal position of the implant. These findings are likely due to the different characteristics of bone-implant interfaces and differences in loading direction and the amount of cortical bone in contact with the implant. Under immediate loading conditions, the load was transmitted toward the apical area of the implant because of frictional contact, and stress was highly concentrated on the thin lateral cortical bones in contact with the sharp implant threads. Under delayed loading conditions, however, stress was concentrated on the crestal cortical bone because of bonded contact and was reduced as the contact surface between the implant and labial cortical bone increased. Thus, positioning an immediately loaded implant in the center or on the palatal side of the ridge resulted in a favorable stress distribution. Long-term stability may also be enhanced by increased contact surface between the implant and cortical bone after osseointegration.

In the present study, an oblique static load of 178 N was applied to the palatal surface of the zirconia crown. As a result, stress was concentrated on the labial side of the crestal cortical bone around the implant platform and neck. These results are similar to those showing that von Mises stresses following oblique loading were highest on the buccal surface of cortical bone around the implant neck [27], suggesting that the type of load is crucial in the distribution and magnitude of stresses on bone surrounding an implant [18]. An oblique load can cause excessive stress on bone surrounding an immediately loaded implant *via* bending moment. Because oblique loads are closely associated with negative outcomes, including marginal bone loss, failure of osseointegration, and damage to the

implant or prosthetic components, careful occlusal examination and adjustments are necessary.

The distribution of stress on the labial bone surface was found to be associated with the labiopalatal position of the implant, with a more labial position associated with higher stress on the labial bone surface. Previous studies, however, found that stress was greater in the marginal region of the labial bone adjacent to the implant and decreased toward the apical area [48, 49]. The labial bone must be able to withstand an occlusal load because of load direction in the anterior maxilla [50]. Excess loads can lead to bone resorption and unfavorable remodeling of labial bone. Therefore, sufficient labial bone thickness around an implant is important for preventing bone resorption and soft tissue contraction [15, 17, 51, 52].

A high degree of displacement was observed on the labial side of the crestal cortical bone around the implant platform, with the distribution of displacement being greater under immediate than under delayed loading conditions. Relative displacement at the bone-implant interface is also called implant micromotion. The magnitude of micromotion is influenced by several factors, including the coefficient of friction at the bone-implant interface, the elastic modulus of the bone, and the osteotomy diameter [47]. Micromotion has a major impact on the primary stability and osseointegration of an immediately loaded implant. Micromotion exceeding a threshold displacement of 150 μm can result in fibrous encapsulation of the implant during the healing process [20, 25], with micromotion less

than 100 μm reported necessary for osseointegration [24]. In the present study, the maximum displacements at the bone-implant interface under immediate and delayed loading conditions were 33.44 μm and 31.88 μm, respectively, lower than the reported thresholds for failure of osseointegration. Our finding that maximum micromotion was similar under immediate and delayed loading conditions may be due to the compressive stress generated in surrounding bone in response to an insertion torque of 35 Ncm under immediate loading conditions [53].

An initial buccal bone thickness of at least 1.5 mm has been reported necessary to reduce bone resorption [54], with bone resorption found to be significantly reduced when labial bone thickness was 1.8–2.0 mm [55]. Furthermore, a labial bone thickness of at least 1.91 mm was optimal in preventing implant failure caused by severe resorption of labial bone [15]. Labial cortical bone is thinner than palatal cortical bone in the anterior maxilla, with cortical bone thickness increasing apically [56]. An anatomic concavity in the apical area on the labial side can increase the risk of perforation during implant placement [57]. Therefore, positioning the implant on the palatal side relative to the center of the crestal cortical bone, thereby ensuring a labial bone thickness of at least 1.5 mm, would result in a better distribution of stress and reduce displacement of surrounding bone under immediate loading conditions.

Use of 3D FEA allowed a determination of the effects of the labiopalatal position of an implant on stress and displacement in the surrounding bone. However, the present study

had limitations, inasmuch as the simplified bone models we used were homogeneous, isotropic, and linearly elastic, differing markedly from a complex and dynamic living bone. Moreover, the geometry of these simplified bone models was different from that of actual bone. Clinical studies are therefore required to confirm the results obtained in the present study.

Future studies should include assessments of the biomechanical effects of immediately loaded implants on surrounding crestal cortical bones of varying thickness, as well as the effects of various implant angles and the dynamic loading resulting from chewing, thereby mimicking more realistic conditions of implantation.

Under immediate loading conditions, stress and displacement were widely distributed toward the apical region along the cortical bone as the implant was positioned more labially, with the magnitudes of stress and displacement depending on the labiopalatal position of the implant. Therefore, the null hypothesis in this study was rejected.

# V. CONCLUSIONS

Labial positioning of an immediately loaded implant increased the area of concentrated stress on the labial side of the surrounding cortical bone. Displacement, both at the bone-implant interface and on the surface of the labial bone, increased as the implant was positioned more labially. Positioning an implant in the center or on the palatal side of the crestal cortical bone of the anterior maxilla under immediate loading conditions were advantageous to stresses and displacements of surrounding bone.

# REFERENCES


[1] Adell R, Lekholm U, Rockler B, Branemark PI. A 15-year study of osseointegrated implants in the treatment of the edentulous jaw. Int J Oral Surg 1981;10:387-416.

[2] Ribeiro FS, Pontes AE, Marcantonio E, Piattelli A, Neto RJ, Marcantonio E, Jr. Success rate of immediate nonfunctional loaded single-tooth implants: immediate versus delayed implantation. Implant Dent 2008;17:109-17.

[3] Ostman PO. Immediate/early loading of dental implants. Clinical documentation and presentation of a treatment concept. Periodontol 2000 2008;47:90-112.

[4] Cochran DL, Morton D, Weber HP. Consensus statements and recommended clinical procedures regarding loading protocols for endosseous dental implants. Int J Oral Maxillofac Implants 2004;19:109-13.

[5] Grutter L, Belser UC. Implant loading protocols for the partially edentulous esthetic zone. Int J Oral Maxillofac Implants 2009;24:169-79.

[6] Piattelli A, Corigliano M, Scarano A, Costigliola G, Paolantonio M. Immediate loading of titanium plasma-sprayed implants: an histologic analysis in monkeys. J Periodontol 1998;69:321-7.

[7] Jaffin RA, Kumar A, Berman CL. Immediate loading of implants in partially and fully edentulous jaws: a series of 27 case reports. J Periodontol 2000;71:833-8.

[8] Donati M, La Scala V, Billi M, Di Dino B, Torrisi P, Berglundh T. Immediate functional loading of implants in single tooth replacement: a prospective clinical multicenter study. Clin Oral Implants Res 2008;19:740-8.

[9] den Hartog L, Raghoebar GM, Stellingsma K, Vissink A, Meijer HJ. Immediate loading of anterior single-tooth implants placed in healed sites: five-year results of a randomized clinical trial. Int J Prosthodont 2016;29:584-91.

[10] Mangano C, Raes F, Lenzi C, Eccellente T, Ortolani M, Luongo G, Mangano F. Immediate Loading of Single Implants: A 2-Year Prospective Multicenter Study. Int J Periodontics Restorative Dent 2017;37:69-78.

[11] Al-Sabbagh M. Implants in the esthetic zone. Dent Clin North Am 2006;50:391-407.

[12] Buser D, Martin W, Belser UC. Optimizing esthetics for implant restorations in the anterior maxilla: anatomic and surgical considerations. Int J Oral Maxillofac Implants 2004;19:43-61.

[13] Scutella F, Weinstein T, Lazzara R, Testori T. Buccolingual implant position and vertical abutment finish line geometry: two strictly related factors that may influence the implant esthetic outcome. Implant Dent 2015;24:343-8.

[14] Evans CD, Chen ST. Esthetic outcomes of immediate implant placements. Clin Oral Implants Res 2008;19:73-80.

[15] Cho YB, Moon SJ, Chung CH, Kim HJ. Resorption of labial bone in maxillary anterior implant. J Adv Prosthodont 2011;3:85-9.

[16] Qahash M, Susin C, Polimeni G, Hall J, Wikesjo UM. Bone healing dynamics at buccal peri-implant sites. Clin Oral Implants Res 2008;19:166-72.

[17] Merheb J, Quirynen M, Teughels W. Critical buccal bone dimensions along implants. Periodontol 2000 2014;66:97-105.

[18] Hsu ML, Chen FC, Kao HC, Cheng CK. Influence of off-axis loading of an anterior maxillary implant: a 3-dimensional finite element analysis. Int J Oral Maxillofac Implants 2007;22:301-9.

[19] Lee JS, Lim YJ. Three-dimensional numerical simulation of stress induced by different lengths of osseointegrated implants in the anterior maxilla. Comput Methods Biomech Biomed Engin 2013;16:1143-9.

[20] Pessoa RS, Coelho PG, Muraru L, Marcantonio E Jr, Vaz LG, Vander Sloten J, Jaecques SV. Influence of implant design on the biomechanical environment of immediately placed implants: computed tomography-based nonlinear three-dimensional finite element analysis. Int J Oral Maxillofac Implants 2011;26:1279-87.

[21] Atieh MA, Shahmiri RA. Evaluation of optimal taper of immediately loaded wide-diameter implants: a finite element analysis. J Oral Implantol 2013;39:123-32.

[22] Misch CE, Suzuki JB, Misch-Dietsh FM, Bidez MW. A positive correlation between occlusal trauma and peri-implant bone loss: literature support. Implant Dent 2005;14:108-16.

[23] Pilliar RM, Lee JM, Maniatopoulos C. Observations on the effect of movement on bone ingrowth into porous-surfaced implants. Clin Orthop Relat Res 1986;208:108-13.

[24] Brunski J. Avoid pitfalls of overloading and micromotion of intraosseous implants. Dent Implantol Update 1993;4:77-81.

[25] Winter W, Klein D, Karl M. Effect of model parameters on finite element analysis of micromotions in implant dentistry. J Oral Implantol 2013;39:23-9.

[26] Borie E, Orsi IA, Noritomi PY, Kemmoku DT. Three-dimensional finite element analysis of the biomechanical behaviors of implants with different connections, lengths, and diameters placed in the maxillary anterior region. Int J Oral Maxillofac Implants 2016;31:101-10.

[27] Ding X, Zhu XH, Liao SH, Zhang XH, Chen H. Implant-bone interface stress distribution in immediately loaded implants of different diameters: a three-dimensional finite element analysis. J Prosthodont 2009;18:393-402.

[28] Lee JS, Cho IH, Kim YS, Heo SJ, Kwon HB, Lim YJ. Bone-implant interface with simulated insertion stress around an immediately loaded dental implant in the anterior maxilla: a three-dimensional finite element analysis. Int J Oral Maxillofac Implants 2012;27:295-302.

[29] Chu CM, Hsu JT, Fuh LJ, Huang HL. Biomechanical evaluation of subcrestal placement of dental implants: in vitro and numerical analyses. J Periodontol 2011;82:302-10.

[30] Rismanchian M, Askari N, Shafiei S. The effect of placement depth of platform-switched implants on periimplant cortical bone stress: a 3-dimensional finite element analysis. Implant Dent 2013;22:165-9.

[31] Misch CE. Density of bone: effect on treatment plans, surgical approach, healing, and progressive boen loading. Int J Oral Implantol 1990;6:23-31.

[32] Bal BT, Caglar A, Aydin C, Yilmaz H, Bankoglu M, Eser A. Finite element analysis of stress distribution with splinted and nonsplinted maxillary anterior fixed prostheses supported by zirconia or titanium implants. Int J Oral Maxillofac Implants 2013;28:e27-38.

[33] Verri FR, Santiago Júnior JF, Almeida DA, Verri AC, Batista VE, Lemos CA, Noritomi PY, Pellizzer EP. Three-dimensional finite element analysis of anterior single implant-supported prostheses with different bone anchorages. Scientific World Journal 2015;2015:1-10.

[34] Mellal A, Wiskott HW, Botsis J, Scherrer SS, Belser UC. Stimulating effect of implant loading on surrounding bone. Comparison of three numerical models and validation by in vivo data. Clin Oral Implants Res 2004;15:239-48.

[35] Bholla P, Jo LJ, Vamsi K, Ariga P. Influence of occlusal loading on stress patterns at the bone-implant interface by angulated abutments in the anterior maxilla: A three-dimensional finite-element study. J Dent Implant 2014;4:3-10.

[36] Clelland NL, Lee JK, Bimbenet OC, Brantley WA. A three-dimensional finite element stress analysis of angled abutments for an implant placed in the anterior maxilla. J Prosthodont 1995;4:95-100.

[37] Furhauser R, Mailath-Pokorny G, Haas R, Busenlechner D, Watzek G, Pommer B. Esthetics of flapless single-tooth implants in the anterior maxilla using guided surgery: association of three-dimensional accuracy and pink esthetic score. Clin Implant Dent Relat Res 2015;17:e427-33.

[38] Vermeulen J. The Accuracy of implant placement by experienced surgeons: guided vs freehand approach in a simulated plastic model. Int J Oral Maxillofac Implants 2017;32:617-24.

[39] Javed F, Romanos GE. The role of primary stability for successful immediate loading of dental implants. a literature review. J Dent 2010;38:612-20.

[40] I-Chiang C, Shyh-Yuan L, Ming-Chang W, Sun CW, Jiang CP. Finite element modelling of implant designs and cortical bone thickness on stress distribution in maxillary type IV bone. Comput Methods Biomech Biomed Engin 2014;17:516-26.

[41] Cooper LF, De Kok IJ, Rojas-Vizcaya F, Pungpapong P, Chang SH. The immediate loading of dental implants. Compend Contin Educ Dent 2007;28:216-25.

[42] Malo P, Rangert B, Dvarsater L. Immediate function of Branemark implants in the esthetic zone: a retrospective clinical study with 6 months to 4 years of follow-up. Clin Implant Dent Relat Res 2000;2:138-46.

[43] Ottoni JM, Oliveira ZF, Mansini R, Cabral AM. Correlation between placement torque and survival of single-tooth implants. Int J Oral Maxillofac Implants 2005;20:769-76.

[44] Kong L, Gu Z, Li T, Wu J, Hu K, Liu Y, Zhou H, Liu B. Biomechanical optimization of implant diameter and length for immediate loading: a nonlinear finite element analysis. Int J Prosthodont 2009;22:607-15.

[45] Siadat H, Hashemzadeh S, Geramy A, Bassir SH, Alikhasi M. Effect of offset implant placement on the stress distribution around a dental implant: a three-dimensional finite element analysis. J Oral Implantol 2015;41:646-51.

[46] Baggi L, Cappelloni I, Di Girolamo M, Maceri F, Vairo G. The influence of implant diameter and length on stress distribution of osseointegrated implants related to crestal bone geometry: a three-dimensional finite element analysis. J Prosthet Dent 2008;100:422-31.

[47] Kao HC, Gung YW, Chung TF, Hsu ML. The influence of abutment angulation on micromotion level for immediately loaded dental implants: a 3-D finite element analysis. Int J Oral Maxillofac Implants 2008;23:623-30.

[48] Alikhasi M, Siadat H, Geramy A, Hassan-Ahangari A. Stress distribution around maxillary anterior implants as a factor of labial bone thickness and occlusal load angles: a 3-dimensional finite element analysis. J Oral Implantol 2014;40:37-41.

[49] Yoda N, Zheng K, Chen J, Li W, Swain M, Sasaki K, Li Q. Bone morphological effects on post-implantation remodeling of maxillary anterior buccal bone: A clinical and biomechanical study. J Prosthodont Res 2017;61:393-402.

[50] Qian L, Todo M, Matsushita Y, Koyano K. Effects of implant diameter, insertion depth, and loading angle on stress/strain fields in implant/jawbone systems: finite element analysis. Int J Oral Maxillofac Implants 2009;24:877-86.

[51] Benic GI, Mokti M, Chen CJ, Weber HP, Hammerle CH, Gallucci GO. Dimensions of buccal bone and mucosa at immediately placed implants after 7 years: a clinical and cone beam computed tomography study. Clin Oral Implants Res 2012;23:560-6.

[52] Al-Shabeeb MS, Al-Askar M, Al-Rasheed A, Babay N, Javed F, Wang HL, Al-Hezaimi K. Alveolar bone remodeling around immediate implants placed in accordance with the extraction socket classification: a three-dimensional microcomputed tomography analysis. J Periodontol 2012;83:981-7.

[53] Sotto-Maior BS, Rocha EP, de Almeida EO, Freitas-Júnior AC, Anchieta RB, Del Bel Cury AA. Influence of high insertion torque on implant placement: an anisotropic bone stress analysis. Braz Dent J 2010;21:508-14.

[54] AlTarawneh S, AlHadidi A, Hamdan AA, Shaqman M, Habib E. Assessment of bone dimensions in the anterior maxilla: a cone beam computed tomography study. J Prosthodont 2018;27:321-8.

[55] Chung MP, Wang IC, Chan HL, Wang HL. Evaluation of buccal bone concavity in the esthetic zone: a cadaver study. Implant Dent 2017;26:751-5.

[56] Spray JR, Black CG, Morris HF, Ochi S. The influence of bone thickness on facial marginal bone response: stage 1 placement through stage 2 uncovering. Ann Periodontol 2000;5:119-28.

# TABLES AND FIGURES

Table 1. Classification of the five finite element models used in the present study.

| Model | Position | Labial bone thickness (mm) | | |
|---|---|---|---|---|
| | | Cortical bone | Cancellous bone | Total |
| P2 | 1.0 mm palatally | 0.75 | 1.75 | 2.50 |
| P1 | 0.5 mm palatally | 0.75 | 1.25 | 2.00 |
| C | Center | 0.75 | 0.75 | 1.50 |
| L1 | 0.5 mm labially | 0.75 | 0.25 | 1.00 |
| L2 | 1.0 mm labially | 0.50 | 0.00 | 0.50 |

Table 2. Mechanical properties of the different materials used in the finite element models.

| Material | Young's modulus (GPa) | Poisson's ratio |
|---|---|---|
| Cortical bone | 13.7 | 0.3 |
| Cancellous bone | 1.37 | 0.3 |
| Titanium alloy (implant, abutment, screw) | 110 | 0.35 |
| Zirconia (crown) | 200 | 0.31 |

Table 3. Maximum von Mises stresses (MPa) at bone-implant interfaces of surrounding bone under delayed and immediate loading conditions.

| Model | Delayed loading | | Immediate loading | |
|---|---|---|---|---|
| | Cortical bone | Cancellous bone | Cortical bone | Cancellous bone |
| P2 | 157.57 | 11.87 | 306.34 | 29.80 |
| P1 | 155.89 | 12.67 | 149.56 | 27.59 |
| C | 157.26 | 13.94 | 133.82 | 23.68 |
| L1 | 131.16 | 15.75 | 160.51 | 22.47 |
| L2 | 80.22 | 5.20 | 186.71 | 22.34 |

Table. 4. Maximum von Mises stresses (MPa) at the surfaces of labial bone under delayed and immediate loading conditions.

| Model | Delayed loading | Immediate loading |
|---|---|---|
| P2 | 18.87 | 22.76 |
| P1 | 21.46 | 26.26 |
| C | 21.89 | 32.15 |
| L1 | 30.15 | 41.40 |
| L2 | 45.01 | 53.31 |

Table 5. Maximum displacements (μm) at bone-implant interfaces of surrounding bone under delayed and immediate loading conditions.

| Model | Delayed loading | Immediate loading |
|---|---|---|
| P2 | 27.48 | 26.93 |
| P1 | 27.85 | 27.69 |
| C | 28.38 | 28.51 |
| L1 | 29.39 | 30.49 |
| L2 | 31.88 | 33.44 |

Table 6. Maximum displacements (μm) at the surfaces of labial bone under delayed and immediate loading conditions.

| Model | Delayed loading | Immediate loading |
|---|---|---|
| P2 | 19.47 | 19.99 |
| P1 | 21.19 | 21.85 |
| C | 23.67 | 24.42 |
| L1 | 27.32 | 28.05 |
| L2 | 31.97 | 33.46 |

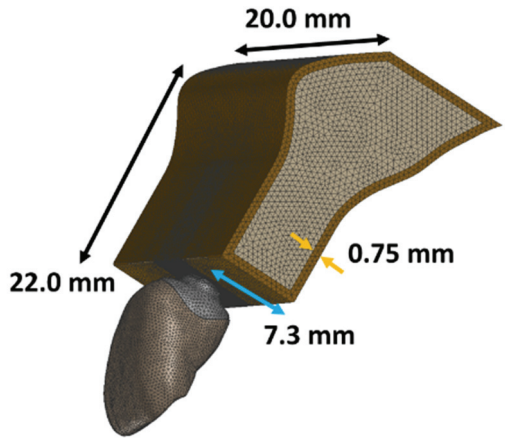


Fig. 1. Dimensions of the 3D finite element bone model used in this study.

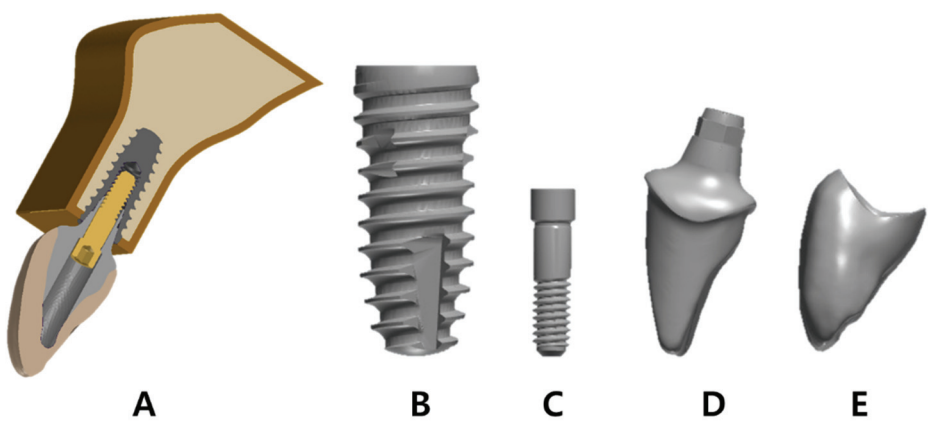


Fig. 2. Solid models used in this study. (A) Labiopalatal cross section of the simplified bone model including components, (B) Implant, (C) Abutment screw, (D) Customized abutment, and (E) Zirconia crown.

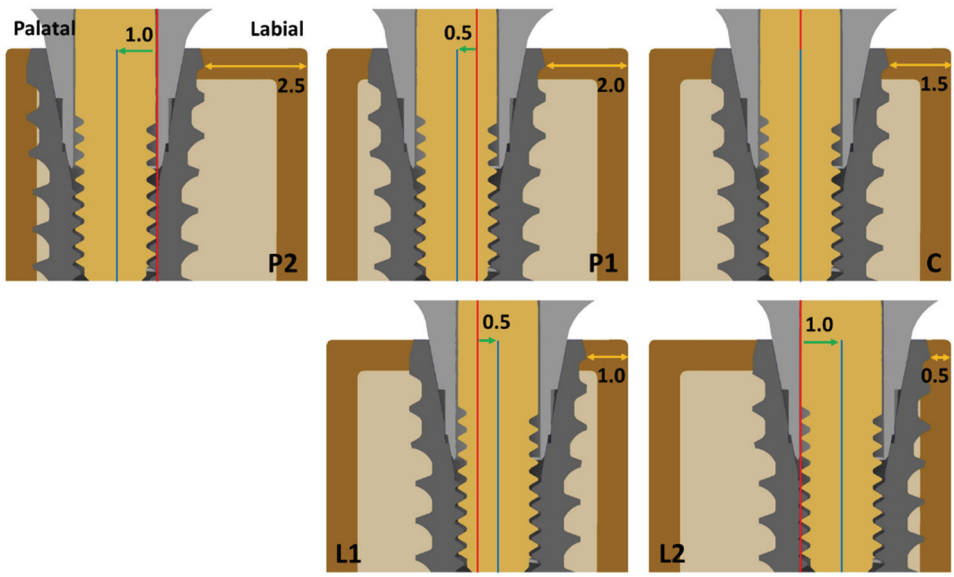


Fig. 3. Representative illustrations of the finite element models. The green arrows indicate the distances (mm) between the central axis of the implant (blue line) and the longitudinal axis of the bone model (red line). The double yellow arrows indicate the distances between the implant and the outer surface of the labial bone.

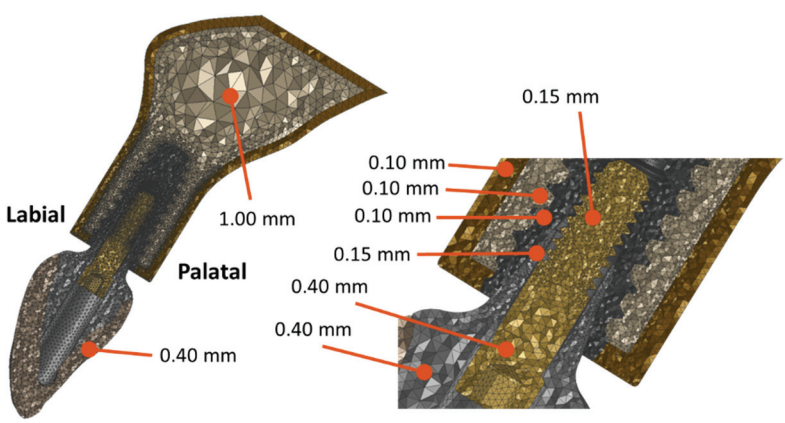


Fig. 4. Mesh creation of the finite element model with tetrahedral elements of various sizes.

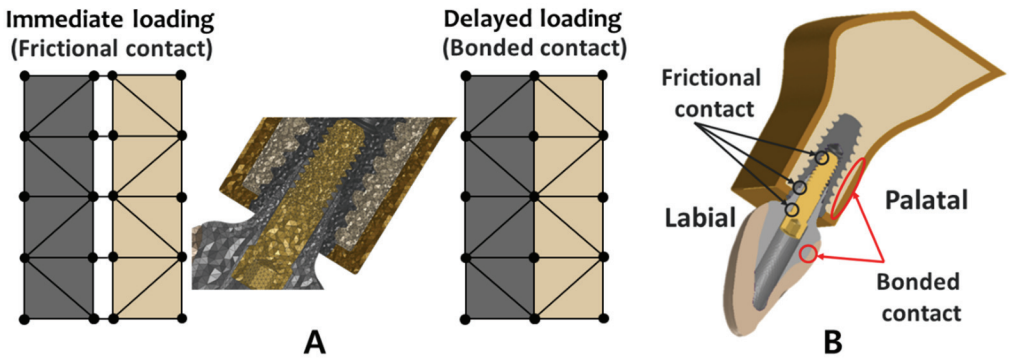


Fig. 5. Contact conditions of the finite element model. (A) Bone-implant interface, (B) Cortical bone-cancellous bone interface and components of the implant.

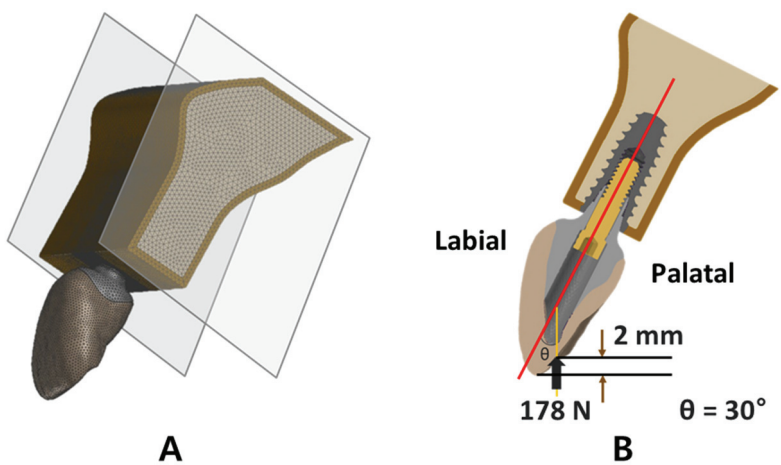


Fig. 6. Boundary and loading conditions. (A) Boundary conditions included constraints of the six degrees of freedom, (B) Application of an oblique static load of 178 N at a 30° angle to the central axis (red line) of the implant.

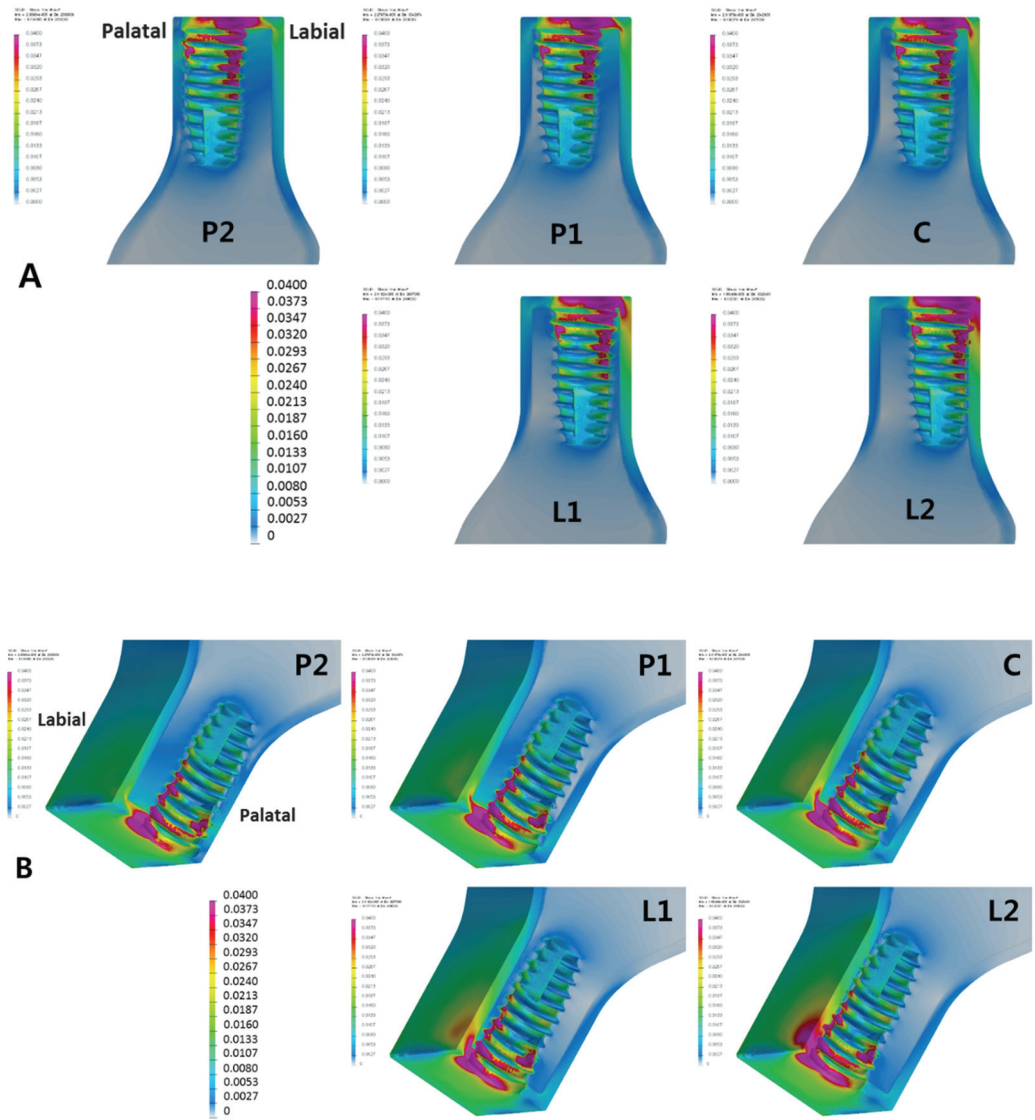


Fig. 7. The von Mises stress distributions of surrounding bone under conditions of delayed loading. (A) Labiopalatal cross sectional view, (B) Isometric view.

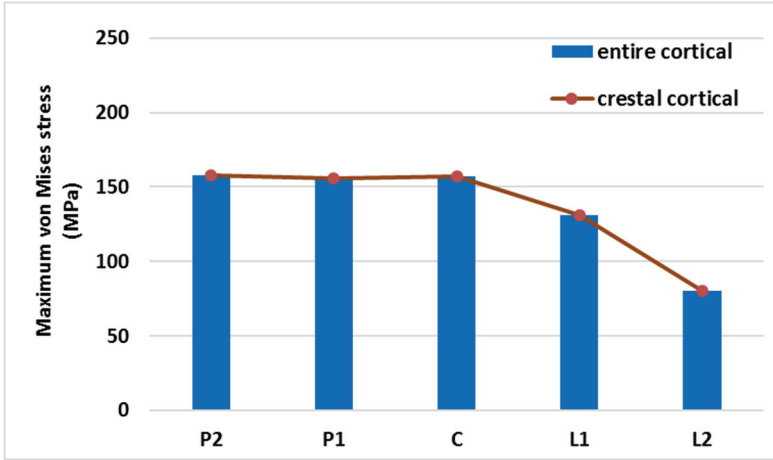


Fig. 8. Maximum von Mises stresses at the bone-implant interface in the entire and crestal cortical bone under conditions of delayed loading.

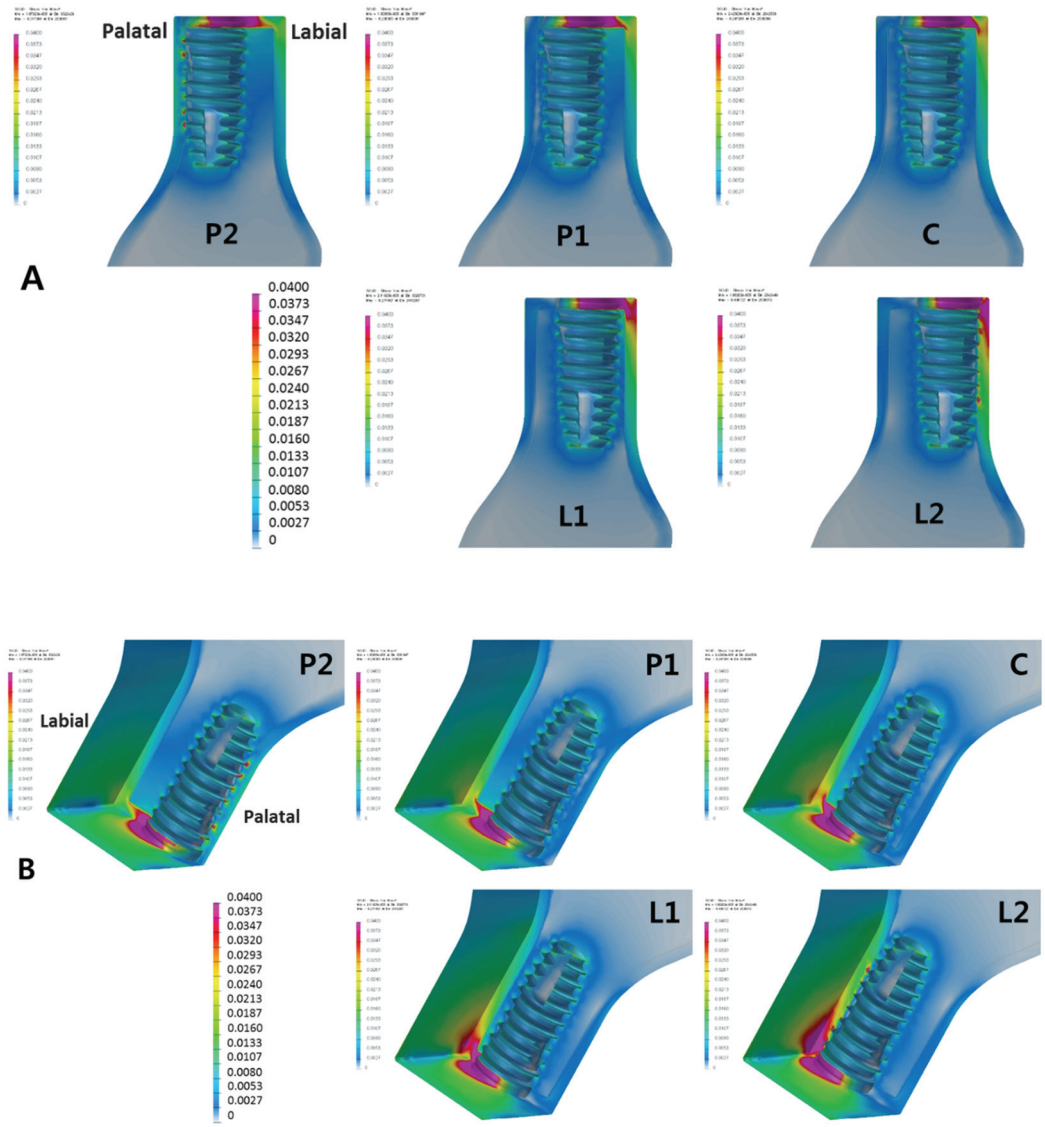


Fig. 9. The von Mises stress distributions of surrounding bone under conditions of immediate loading. (A) Labiopalatal cross sectional view, (B) Isometric view.

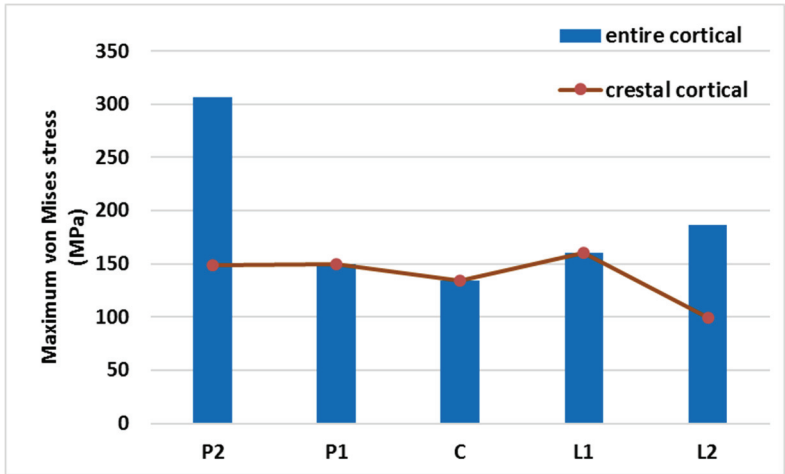


Fig. 10. Maximum von Mises stresses at the bone-implant interface in the entire and crestal cortical bone under conditions of immediate loading. The maximum stresses were the same in the P1, C, and L1 models.

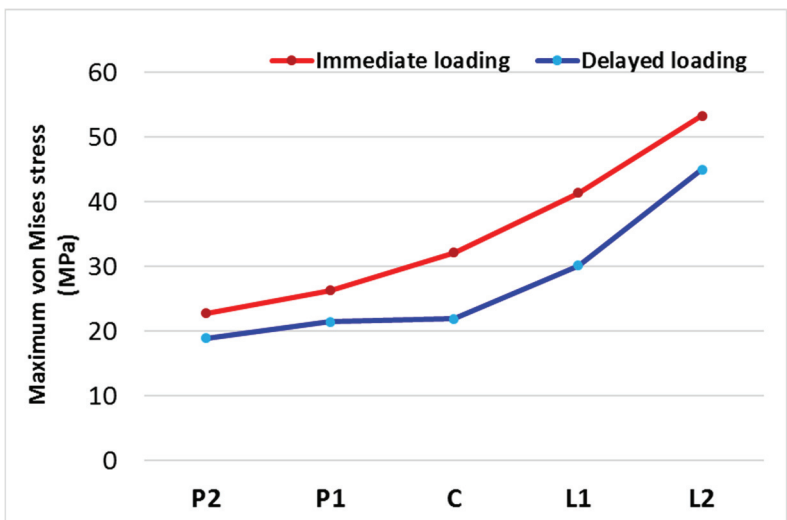


Fig. 11. Maximum von Mises stress values on the labial bone surface. At each implant position, the immediate loading models showed higher maximum stress than the delayed loading models.

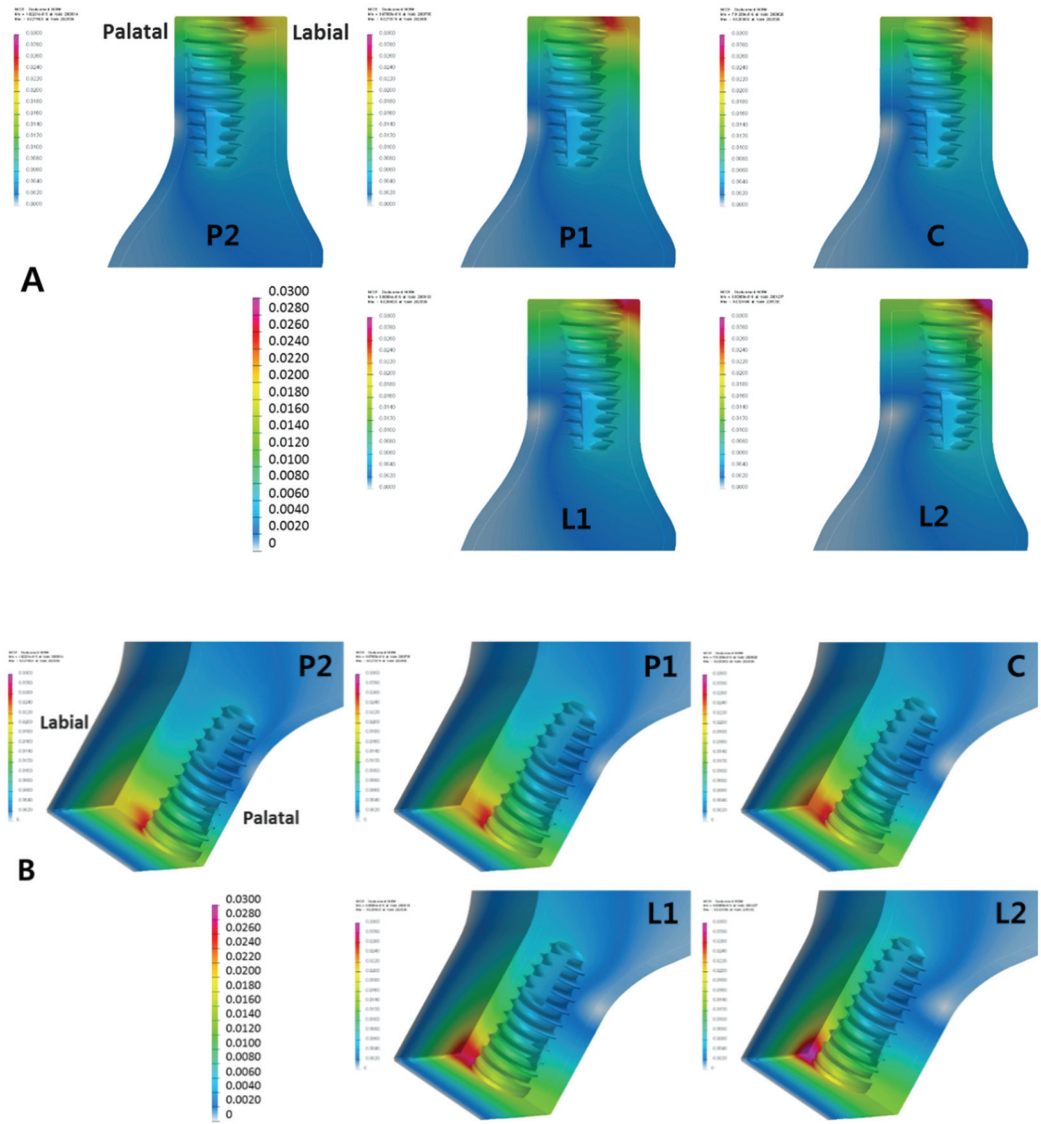


Fig. 12. Displacement distribution of the surrounding bone under delayed loading conditions. (A) Labiopalatal cross sectional view, (B) Isometric view.

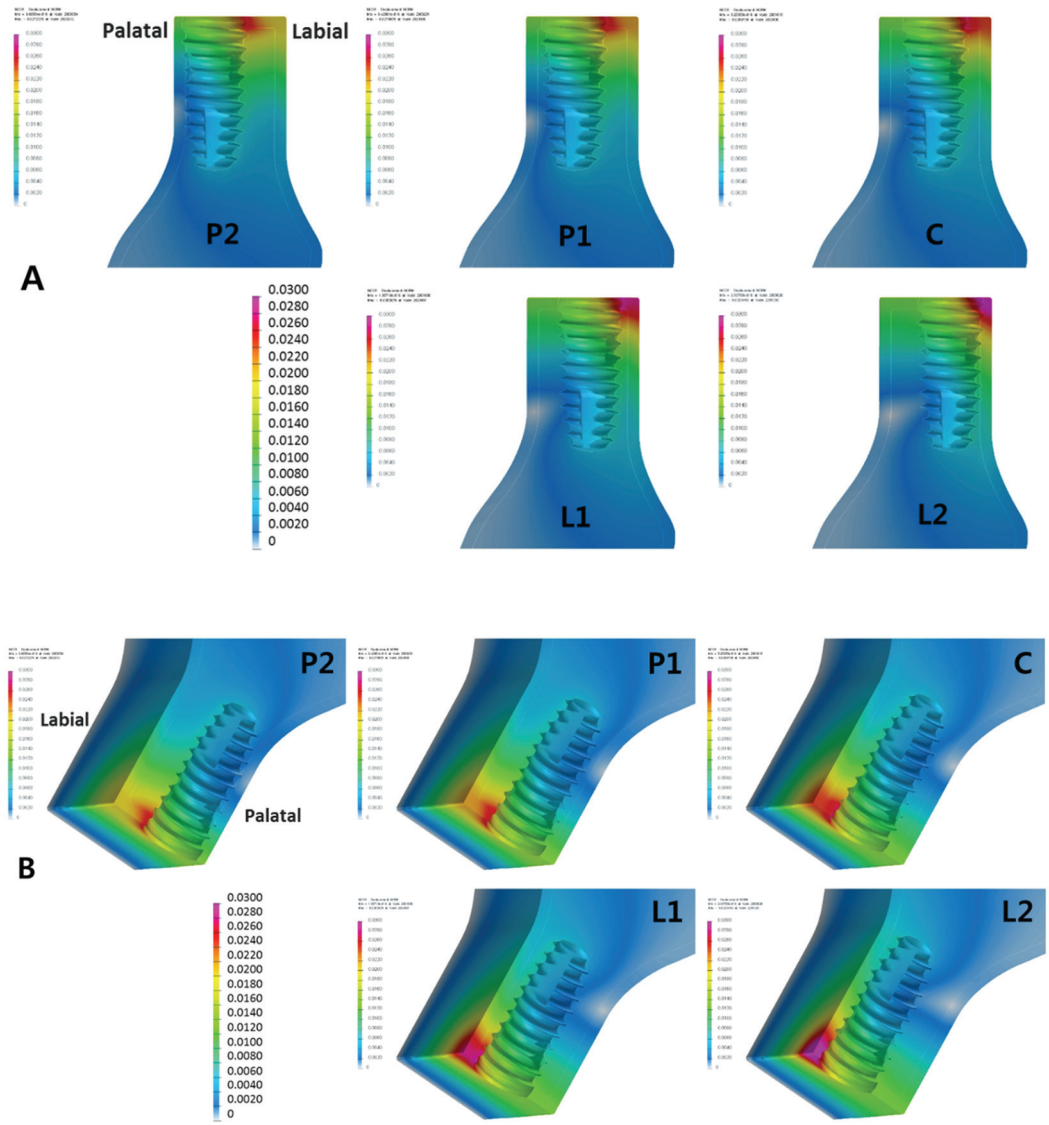


Fig. 13. Displacement distribution of the surrounding bone under immediate loading conditions. (A) Labiopalatal cross sectional view, (B) Isometric view.

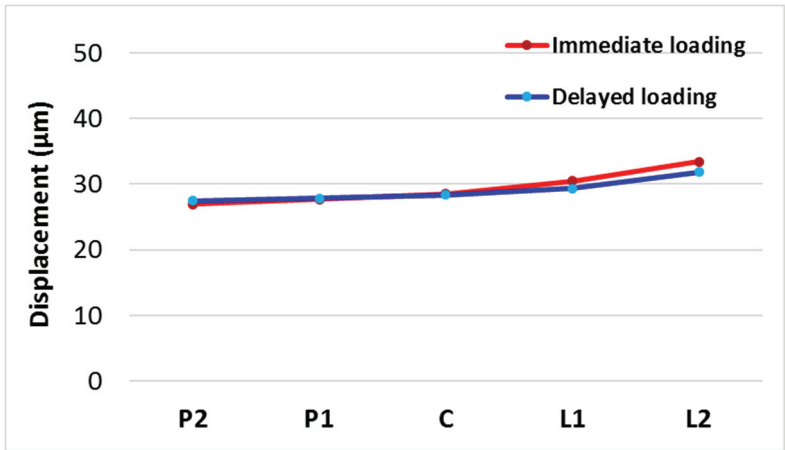


Fig. 14. Maximum displacements at the bone-implant interface.

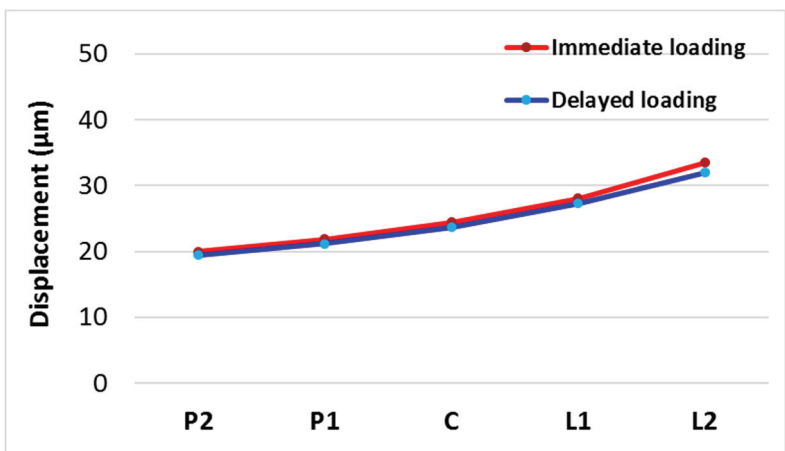


Fig. 15. Maximum displacements at the labial bone surface.

국문초록

# 임플란트의 순구개 위치가 골의 응력과 변위에 미치는 영향: 3 차원 유한요소분석

서울대학교 대학원 치의과학과 치과보철학 전공

(지도교수 한 중 석)

**박 철 우**

**연구 목적:** 본 연구의 목적은 삼차원 유한요소분석을 이용하여 상악 전치부에서 즉시부하 임플란트의 순구개 위치가 주변 골의 응력과 변위에 미치는 영향을 알아보는 것이다.

**재료 및 방법:** 내부 연결형 임플란트(4.0 X 10.0 mm), 맞춤형 지대주, 지대주 나사, 시멘트 유지형 중절치 지르코니아 크라운으로 구성된 5 개의 단순화 삼차원 유한요소 모델을 제작하였다. 임플란트를 5 군데 다른 순구개 위치인, 치조정 피질골의 중심에서 구개측으로 0.5 mm (P1) 와 1.0 mm (P2), 중심

(C), 그리고 중심에서 순측으로 0.5 mm (L1) 와 1.0 mm (L2) 에 식립하였다. 178 N 의 경사진 정하중을 즉시부하 및 지연부하 조건에서 임플란트 장축에 대하여 30°로 지르코니아 크라운의 구개면에 적용하였다. 주변 골의 등가 응력과 변위를 골-임플란트 계면과 순측 골 표면에서 계산하였다.

**결과:** 등가 응력이 주로 임플란트 상단과 경부 주변 치조정 피질골에 집중되었다. 순측 피질골의 응력 분포는 임플란트가 더 순측에 식립될수록 증가하였다. 해면골의 응력은 지연부하보다 즉시부하 조건에서 더 균등하게 분포하였다. 피질골의 최대 응력은 순측 골 표면에서 임플란트의 순구개 위치와 규칙적인 관계가 있었지만 골-임플란트 계면에서는 그렇지 않았다. 즉시부하 조건에서, P1 과 C 모델은 피질골에서 양호한 응력과 변위 양상을 보였다. 최대 변위는 임플란트가 순측에 식립될수록 증가하였고, 즉시부하와 지연부하 조건 사이에 차이가 거의 없었다. 즉시부하 조건에서 골-임플란트 계면의 최대 변위는 33.44 μm 였다.

**결론:** 임플란트의 순구개 위치는 상악 전치부에서 주변 골의 등가 응력과 변위에 영향을 주었다. 치조정 피질골의 중심 또는 구개측에서 임플란트의 즉시부하는 주변 골에 양호한 응력과 변위 양상을 나타냈다.

**주요어:** 치과용 임플란트, 즉시부하, 순구개 위치, 유한요소분석

**학 번:** 2011-31175